Pipe-wall-thinning measurement technique employing electromagnetic acoustic resonance and its application to power plant piping

TAKAGI Toshiyuki[1,2], **URAYAMA Ryoichi**[1], **UCHIMOTO Tetsuya**[1,2], **and SUN Hongjun**[1]

1. Institute of Fluid Science, Tohoku University, 2-1-1 Katahira, Aoba-ku, Sendai 980-8577, Japan (takagi@ifs.touhoku.ac.jp)
2. ELyTMaX, UMI3757, CNRS–Université de Lyon–Tohoku University, International Joint Unit, Tohoku University, 2-1-1 Katahira, Aoba-ku, Sendai, 980-8577, Japan

Abstract: In power plants, the acceleration of corrosion thinning in piping from aging is of concern. Maintaining the safety of plant systems from such deterioration is desired. An inspection method of pipe-wall thinning is proposed using an electromagnetic acoustic transducer and has been studied for its applicability to actual piping. The inspection through measurement and signal processing uses the electromagnetic acoustic resonance method and superposition of the n-th compression. Measurement at a BWR simulated equipment was performed under a high temperature environment and the applicability of the method was evaluated. In this study the method of measuring wall thickness was applied and evaluated the performance of the pipes iof the actual plant where flow-accelerated corrosion had occurred. In addition, the pipe thickness was measured at a power plant during operation and monitored pipe-wall thickness during the plant decommissioning to evaluate the applicability of the used measurement method.

Keyword: pipe wall thickness inspection; electromagnetic acoustic resonance method; monitoring system; power plant

1 Introduction

In piping systems of power plants, pipe-wall thickness becomes thin due to corrosion in pipes through which water and steam flow. Typical pipe thinning is caused by flow-accelerated corrosion (FAC) or liquid-droplet impingement (LDI) erosion. As the operating years of a plant increases, the thickness gradually decreases. If this reduction accelerates, a serious accident such as a rupture of the pipe may occur. For this reason, in a power plant, wall thickness measurements are performed periodically and the life expectancy remaining of the pipe in relation to the minimum wall thickness determined at the time of its design is obtained.

In general, the methods used in wall thickness inspections employ an ultrasonic thickness gauge requiring a contact medium. Alternatively, an electromagnetic acoustic transducer (EMAT) may be used and moreover it does not require a contact medium for measurements [1-2]. However, there has been no report of its application to pipes in actual power plants for monitoring of thickness.

An inspection proposal was put forward for which measurements are performed using an EMAT based on electromagnetic acoustic resonance (EMAR) and signal processing was done using the method of superposition of the n-th compression (SNC). Moreover, the inspection was applied to simulated piping specimen and was studied to evaluate the applicability of the proposal.

First, for on-line monitoring, we applied the EMAR system to measure thickness using the pipe-wall thinning test equipment under high-temperature environments equivalent to a real plant and evaluated its applicability. The following results were obtained [3-4].

1) At the high temperature of 165 °C, it was possible to evaluate the decrease in thickness with elapsed time and confirm the difference in wall thinning rate under three different water flow conditions.

Received date: September 20, 2018

2) The difference between the thickness readings via EMAR and from a microscope was 0.06mm at the end of the test.
3) From the results of the SNC analysis waveforms, the attenuation of the SNC peak and multiple SNC peaks representing the change in shape of the bottom surface were observed after thickness reduction.

Next, the EMAR system was applied in wall-thickness inspections of piping in the cooling system of Unit 2 at the Tsuruga Nuclear Power Station. An assessment of the applicability was performed in a comparison with measurement results using the ultrasonic thickness gauge. From SNC signal processing, the shape of the bottom surface was determined from the standardized normalized SNC peak value and the half-width-at-peak of a standard test piece used as a reference [4-5].

1) The result did not depend on the diameter of the tube, whether straight or elbow, and its influence on the measured thickness was small. However, there are differences in EMAR and UT (Ultrasonic Testing) results from around welding.
2) If the normalized SNC peak value is larger than 0.15, the mean-square-root error (RMSE) between EMAR and UT are in good agreement by 0.18mm, and the reliability is high. However, if the peak value from normalized SNC is less than 0.05, the difference between the UT and EMAR results increases reaching 3mm.

In this study, the following aspects of actual piping are investigated using the EMAR system.

1) The pipes in which wall thinning have occurred by FAC are measured using the EMAT. Applicability is assessed by comparing the results measured by ultrasonic thickness gage and caliper gauge.
2) Thicknesses of pipes during plant operations are measured and compared with measurement results obtained using the ultrasonic thickness gauge; again applicability is assessed.
3) The EMAR system is applied to the monitoring of pipe-wall thickness in the piping for the spent-fuel-pool circulation cooling system at Fukushima Daiichi Nuclear Power Station Unit 4 in its decommissioning stage, and applicability is assessed.

2 Pipe thinning inspection by EMAR method

2.1 EMAT and EMAR method

EMAT generates ultrasonic waves near the specimen surface by an electromagnetic effect distinct from normal UT, which propagates ultrasonic waves from a probe composed of a piezoelectric element via a medium in contact with the specimen. For this reason, the EMAT is able to make a measurement without contact, and hence the influence of paint and irregularities on the surface of the specimen is small.

The EMAT consists of a permanent magnet and a coil. When an electric current passes through the coil placed on a conductive specimen, an eddy current is induced near the specimen surface creating a magnetic field in the opposite direction to the magnetic field formed by the current.

Also, because of the interaction between the eddy current and the static magnetic field from the permanent magnet, a Lorentz force is generated in the specimen. When an alternating current flows through the coil, a shear wave is generated by the Lorentz force that periodically changes and propagates in the specimen.

However, when the specimen is a magnetic material, not only the Lorentz force but also the magnetostrictive force arising from the magnetostrictive effect is generated by the interaction between the magnetic induction magnetic field due to the eddy current and the magnetic flux density by the permanent magnet. For a ferromagnetic material, both the Lorentz and magnetostrictive forces act, but the former dominates the latter [6].

When the thickness of the specimen is an integral multiple of the wavelength, resonance occurs because of phase matching of the incident wave and the reflected wave; the received signal is then amplified. The EMAR method exploits this phenomenon. Moreover, the resonance frequency is that when the phases of the incident and reflected waves match. The relationship between resonance frequency and thickness is

$$f_n = n \times f_1 = n \times \frac{c}{\lambda} = n \times \frac{c}{2d} \ ,$$

where f_n is the resonance frequency, f_1 fundamental resonance frequency, n resonance order, λ wavelength, c sound velocity, and d thickness.

If a high-voltage burst wave is transmitted over a certain time duration, an echo is repeatedly heard inside the test piece after the transmission has stopped and when resonance occurs in the specimen. The transmission frequency is finely swept within the range of the test frequency. Synchronous detection is performed for each swept frequency, and the peak of the amplitude intensity is obtained. Moreover, the fundamental resonance frequency can be specified from the frequency between the peaks [7-8].

2.2 SNC method

The SNC method is the signal-processing method that exploits those resonance frequencies that periodically appear when the resonance frequency is an integral multiple [5]. The fundamental resonance frequency is identified by determining the peak of the fundamental resonance frequency from the received signal with a small SN ratio or with multiple peaks by compressing the frequency axis to 1/n and overlapping the two signals. The resonance spectrum of a carbon steel pipe with a thickness of 5mm is plotted (Fig.1) using EMAR measurements, along with the result of SNC signal processing (Fig.2).

When the n-th resonance frequency f_n is compressed by $1/n$, the fundamental resonance frequency f_1 is obtained. That is, the maximum peak value of the resonance frequency SNC spectrum, obtained by compressing the frequency axis by $1/n$ and overlapping the signals, corresponds to the fundamental resonance frequency f_1. The thickness obtained from the SNC method is then calculated using [5]

$$f_1 = \arg\max_f \left\{ \sum_n x(nf) \right\} \quad ,$$

$$d = \frac{c}{2f_1} \ ,$$

where $x(f)$ is the SNC spectrum intensity.

However, the resonance frequency changes according to thickness and speed of sound, and the range of the order n of the resonance frequency included in the test frequency range changes. For example, when the wall thickness of the test pipe is 5.0mm and the speed of sound is 3240 m/s, the resonance frequency is 324 kHz, and the degree of resonance is an integer ranging from 5 to 10 if the test frequency range is 1.5 to 3.5 MHz.

The frequency axis of the EMAR measurement result (Fig.1) is compressed to 1/5 to 1/10 and added together to emphasize the peak at the fundamental resonance frequency; the fundamental resonance frequency then becomes clear (Fig.2). Here, the SNC spectrum intensity is averaged by the number of order ranges to be added.

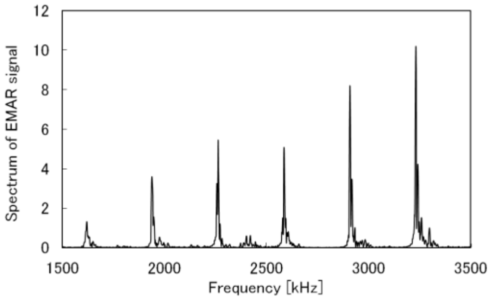

Fig. 1 EMAR signal.

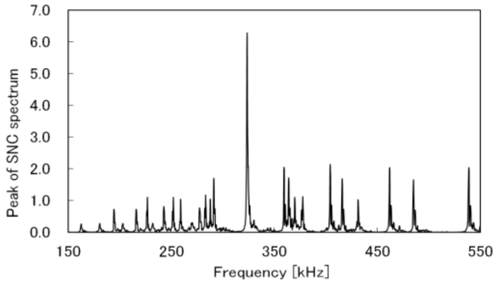

Fig. 2 Result of SNC signal processing.

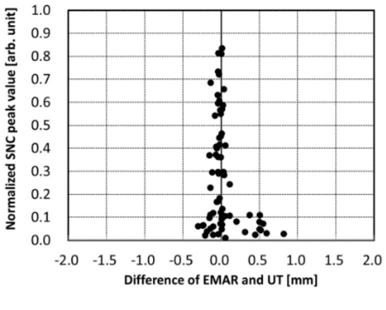

Fig. 3 Relationship between normalized SNC peak value and the difference in the EMAR and UT thicknesses [5].

2.3 Thinning evaluation parameter

2.3.1 Normalized SNC peak value

The maximum peak value in Fig.2 is the SNC peak value. To normalize the SNC peak value, the measurement conditions of the EMAR method (such as material, transmission signal, gain, test frequency range, and sweep frequency) are set to the same initial conditions.

Moreover, a flat plate of the same material as the reference specimen to be measured is prepared as a reference specimen, and the SNC peak value of the measurement result is normalized to 1 [5]. As a relative value, the value is referred to as the normalized SNC peak value.

Figure 3 shows the relationship between the SNC peak values and the difference in the EMAR and UT thicknesses obtained. This is the result obtained by the EMAR system during the wall thickness inspection of piping in the cooling system of Unit 2 of the Tsuruga Nuclear Power Station [5].

If the normalized SNC peak value is larger than 0.15, the RMSE of the difference between EMAR and UT agrees well with 0.2mm or less, and the reliability is high. However, if the normalized SNC peak value is less than 0.05, the difference between the UT and EMAR results tends to be large [5].

2.3.2 FWHM (Full Width Half Maximum)

In specifying the fundamental resonance frequency, the normalized SNC peak value is an important value used for calculating thickness. Therefore, it is necessary to evaluate how reliable the peak value is. Related to the evaluation of the reliability is the full-width at half-maximum (FWHM), which is the interval between two frequency values before and after the peak at half the normalized SNC peak value (Fig.4). This frequency value obtained from the FWHM determines the range of estimated wall thickness; the difference in the thickness which corresponds to before and after is shown [8].

2.4 Outline of wall thickness measurement by EMAR method

The EMAR system consists of a high-power pulsar receiver (RPR-4000 RITEC), a preamplifier (PASJ-0.1-20 RITEC) that amplifies the received signal, a wideband decade filter (FV-628B NF), an oscilloscope (DPO 4104, TEKTRONIX) for waveform observations and data acquisition, and a PC for storing and analyzing waveform data.

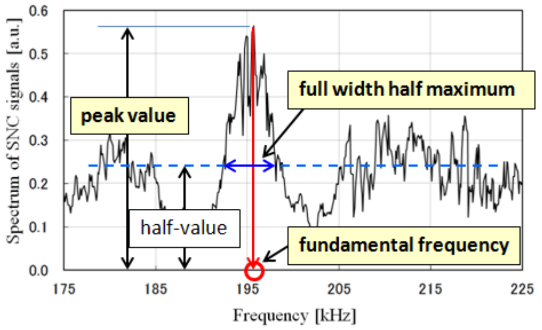

Fig. 4 Example of FWHM.

The transmission coil and the reception coil of the EMAT are separately constructed. To reduce the influence of scattering of the ultrasonic waves because of the change in shape of the bottom surface, the diameter of the transmission coil is set to 10mm and the incident area is made small. Moreover, the attenuation of the received signal is reduced by setting the diameter of the receiving coil to 20mm. The wire diameter of the coil is 0.12mm, the number of turns of the transmitting coil is 40, and that of the receiving coil is 80. The permanent magnet is used by combining two samarium cobalt magnets of dimension 10mm (width), 20mm (length), and 20mm (excitation direction) and having a high Curie temperature. The test frequency range is set to 1.5 to 3.5 MHz and the sweep interval is set to 5 kHz. Fourier analysis processing is applied to the received signal data, and synchronous detection is performed by frequency increments of 1 kHz to obtain the fast Fourier transform (FFT) spectrum.

3 Evaluation of wall thickness of piping of thermal power plant

3.1 Outline of an actual pipe test piece

The specimens are bent pipes of carbon steel that were used in the thermal power plant and featured FAC thinning through aged deterioration. The outer and inner diameter of the pipes were 139.8mm and 126.6 mm, and the nominal wall thickness was 6.6mm (thickness tolerance ± 12.5%). The operating conditions were an internal fluid temperature of 128 C and a flow rate of 8.55 m/s (both at the rated load and design value for the flow velocity)[9]. These pipes were either dorsal or ventral and shall be referred to as such. Figure 5 is a photo showing the appearance of a ventral pipe specimen. The dorsal test piece was divided into 12 segments for surface examination.

Fig. 5 Photo of the appearance of the ventral specimen.

3.2 Measurement result of ventral specimen

Plots were made of the wall thickness distribution obtained from UT measurements (Fig.6) and the EMAR and UT thickness correlation (Fig.7). The measured thicknesses ranged from 4.5mm to 6.4mm, which is thinner than the nominal wall thickness of 6.6mm. The wall thickness is maximum near the100-mm mark downstream from the inlet; at the inlet and outlet of the bent pipe, the wall was thin.

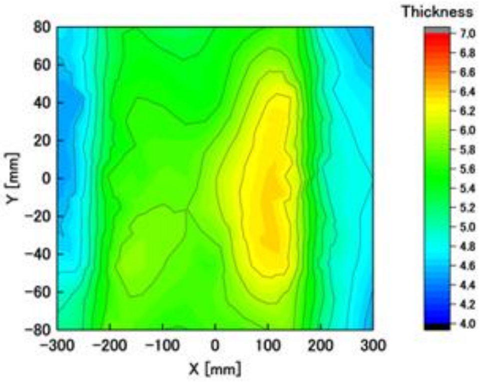

Fig. 6 Distribution by UT thickness of ventral specimen.

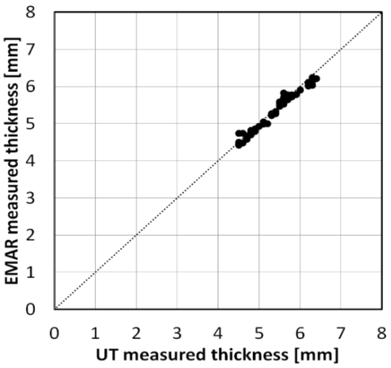

Fig. 7 EMAR and UT thickness correlation at ventral specimen [10].

The maximum difference between EMAT and UT wall thicknesses was 0.27mm, and the root mean square of this difference was 0.09mm. The EMAR method yields the same degree of accuracy as the UT method.

From a typical photo of the ventral specimen (Fig.8), the inner surface is relatively smooth, although pitting is evident with indentations of 2–3mm in size and 0.1–0.5 mm in depth. From the distribution of the UT wall thickness (Fig.6), the change in thickness is gradual on the whole. Hence, the minimum wall thickness of the indentations is considered unmeasurable and difficult to measure using the UT and EMAR methods.

Fig.8 Photo of the inner surface of the ventral specimen.

3.3 Measurement result of the dorsal specimen

The UT thickness distribution of the dorsal specimen (Fig.9) shows a measured range of thickness of 2.3–5.2mm, which is thinner than the nominal wall thickness of 6.6mm, the pipe on the whole being thin. In particular, wall thinning downstream was confirmed over a large range of 100mm along the X-axis direction. Also, there is thinning in the circumferential direction (Y axis) above the flow direction (X axis) at –150mm.

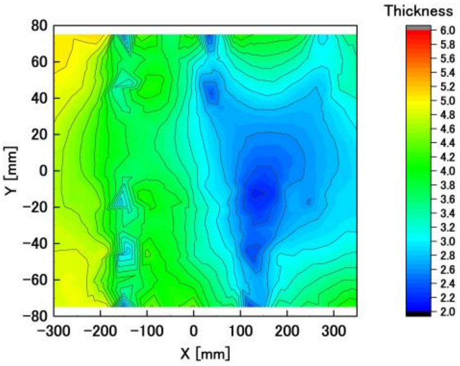

Fig. 9 Distribution of the UT thickness of dorsal specimen.

From the correlation between the measured EMAR and UT thicknesses (Fig.10), the difference in thickness is large when the measured thickness is less than 4.5mm (nominal wall thickness 6.6mm) where a reduction in thickness is seen to be advanced. The maximum difference between EMAR and UT wall thicknesses is 1.08mm, the root mean square of the difference being 0.27mm.

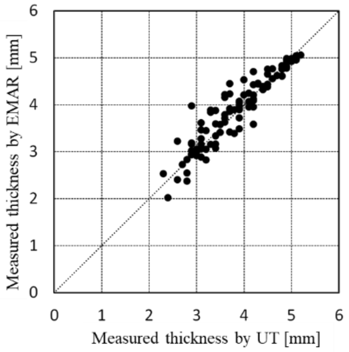

Fig. 10 Correlation between the measured EMAR and UT thicknesses of dorsal specimen [10].

The correlations between the EMAR and UT difference and two parameters, the normalized SNC peak value (Fig.11, upper panel) and. the FWHM (Fig.11, lower panel) show that when the normalized SNC peak value is 0.4 or less, a UT wall thickness difference appears and becomes large at 0.1 or less, whereas FWHM varies regardless of its value. In addition, compared with the ventral specimen, FWHM is large in value. Even if FWHM is small, there is a difference in UT thickness.

Figure 12 shows the distributions of the normalized SNC peak values and FWHM. The EMAR results show prominently that the normalized SNC peak value decreases and the FWHM increases on the downstream side of the X axis at −100mm.

A typical photo of the inner surface (Fig.13) shows that the indentations from thinning are scattered in the upstream region but do not feature a scale-like shape. In contrast, scaly thinning is evident in the central region downstream. The size of the scales is large in the center of the pipe and relatively small on the downstream side.

The measurement accuracy is good in the thinned region that does not show a scaly knitting shape. Also, even in the region where thinning is heaviest, no large difference in UT thickness is seen. However, the difference is large in the region where the slope, caused by thinning around it, is large. The difference in UT thickness increases by both slope and scaly indents arising from thinning.

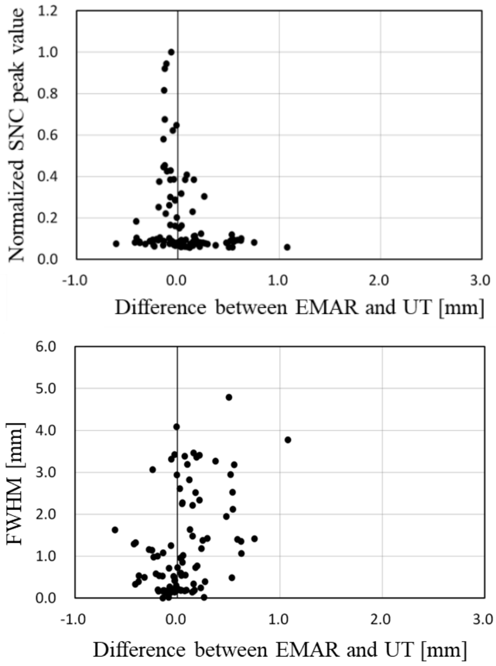

Fig. 11 Correlations between evaluation parameters (upper panel: normalized SNC value, lower panel: FWHM) and the difference between EMAR and UT thicknesses of dorsal specimen.

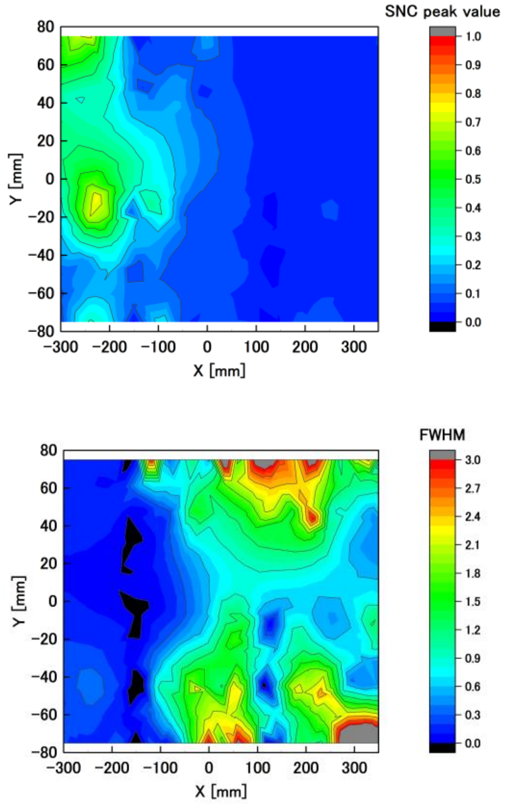

Fig. 12 Distribution of evaluation parameters of dorsal specimen (upper: normalized SNC value, lower: FWHM).

Fig. 13 Photo of the inner surfaces of a dorsal specimen.

3.4 Comparison between caliper gauge and EMAR measurement results

From the correlation between the EMAR measured thickness and the caliper-gauge measured thickness (Fig.14), the maximum difference in wall thickness is 0.79mm (the UT measurement result was 1.08mm), and the RMSE of the difference from the caliper-gauge measurement is 0.24mm (the UT measurement result was 0.27mm).

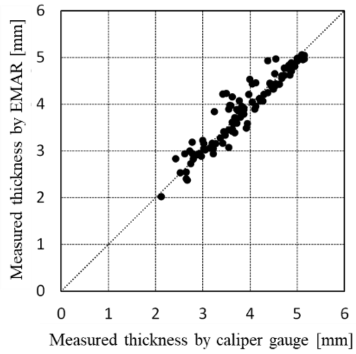

Fig. 14 Correlation between EMAR and caliper gauge of dorsal specimen [10].

Similarly, Fig.15 shows correlations between the EMAR−caliper gauge difference and the normalized SNC peak value (upper panel) and the FWHM (lower). The difference is confirmed at several measured points. From the caliper-gauge measurement, the difference from the EMAR becomes large because the measurement was performed at a deep recess.

4 Measurement of thermal power plant piping during operation by EMAT

4.1 Measurement overview

The EMAR system was applied in measurements to actual piping in a thermal power plant while in operation, and its applicability evaluated. The measurement location was on two straight pipes upstream (horizontal pipe) and downstream (vertical pipe) of an elbow portion at a double water pump outlet, where there are two lines of pipes (A line and B line) at the outlets of two water-system-generator hydrogen-gas coolers. The piping material is carbon steel; the outer diameter of the pipe is 267.4mm with a nominal wall thickness of 9.3mm. The design temperature is 60°C (piping temperature at the time of measurement is roughly room temperature), and the design pressure is 1 MPa.

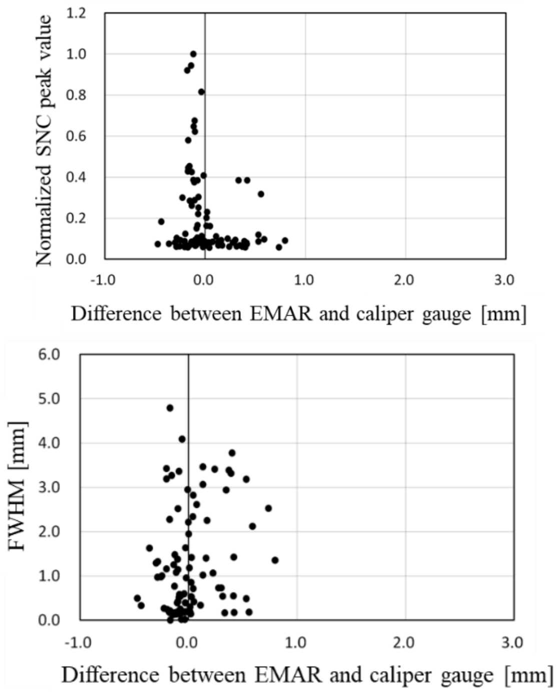

Fig. 15 Correlations between evaluation parameters of dorsal specimen (upper panel: normalized SNC value, lower panel: FWHM) and difference between EMAR and UT.

In addition, the piping surface is not covered with heat insulation material but is painted. The paint was not removed during measurements. The measurement point is located about 50mm away from the weld connecting the straight pipe and the elbow section. There are no deposits or irregularities that affect measurement on the pipes.

For comparison, the wall thickness was measured using an ultrasonic thickness gauge (UDM-570DL, TEITSU DENSHI KENKYUSHO Co. Ltd.), the probe being of T606 type (outer diameter 14mm, 5 Z 6/2 NDT) and the measuring frequency is 5 MHz. However, the UT measurement was performed with a contact medium without removing the paint coating.

From the configuration of the test pipe (Fig.16), the pipe installed horizontally on the upstream side of the elbow section is called the ‘horizontal pipe’; that installed vertically on the downstream side of the elbow section is called the ‘vertical pipe’. The measurement points of the vertical (horizontal) pipe [Fig.17 (18)] are labelled beginning with No.1 located on the dorsal (ventral) side of the elbow pipe and the rest located and labelled Nos. 2, 3, and 4 in a clockwise (anticlockwise) sequence every 90°.

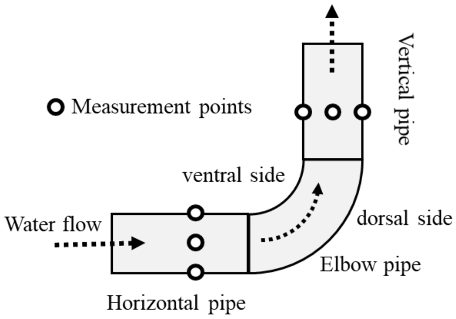

Fig. 16 Outline of the test pipe.

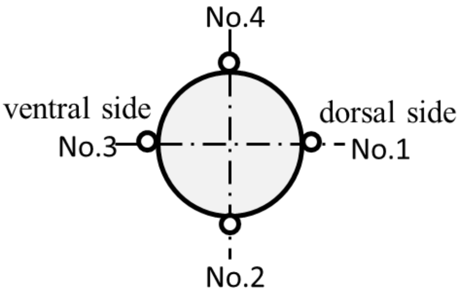

Fig. 17 Measurement points of the vertical pipe.

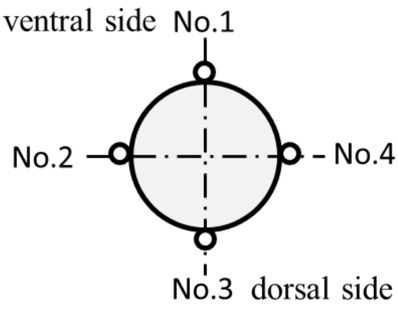

Fig. 18 Measurement points of horizontal pipe.

4.2 Results and discussion

Given the results of the EMAR measurements (Table 1), the signal reliability was judged based on the normalized SNC peak value and FWHM. At location No.3 of the horizontal pipe, the signal amplitude attenuates. The cause of this attenuation is thought to be pipe thinning and the change in the inner surface shape. However, because the wall thickness obtained in the evaluation is not much different from the others, a large reduction in wall thickness does not appear to be the difficulty.

Table 1 Results of thickness measurements

	No.	Normalized SNC peak value	FWHM [mm]	Measured thickness [mm]	Signal reliability
A-Vertical	1	0.37	0.08	8.20	◎
	2	0.38	0.12	8.16	◎
	3	1.00	0.10	7.98	◎
	4	0.42	0.12	8.02	◎
B-vertical	1	0.51	0.10	8.12	◎
	2	0.66	0.08	8.29	◎
	3	0.22	0.16	8.57	◎
	4	0.35	0.11	8.31	◎
A-Horizontal	1	0.18	0.28	8.04	○
	2	0.99	0.10	8.24	◎
	3	0.08	0.65	8.50	▲
	4	0.24	0.15	8.27	○
B-Horizontal	1	0.33	0.16	7.96	◎
	2	0.32	0.13	8.24	◎
	3	0.08	0.30	8.64	△
	4	0.33	0.08	8.24	◎

◎ Good SN ratio
○ Better SN ratio
△ Not good (normalized SNC peak value is 0.1 or less and FWHM 0.5 or less)
▲ Less accurate (normalized SNC peak value is 0.1 or less and FWHM 0.5 or more)

For subsequent periodical inspections, a mark seal for the fixed-point locations for the UT wall thickness measurements was affixed to the pipe surface and painted on it. Therefore, for this current measurement, there is a possibility that it was measured above the seal. In particular, it was later confirmed that a large number of seals were affixed in the measurement region of No. 3 on the horizontal pipe where the SN ratio was small. As there was a variation in thickness indicated, even in UT measurements, an influence by the mark seal is possible.

From the correlation between the EMAR and UT measured thicknesses (Fig.19), there is a difference of −0.3 to −0.8mm, and the UT value is found to be thicker than the EMAR value. The UT thickness was measured from above the paint, so an influence is conceivable. The velocity of sound in epoxy paint is about 2.5 times slower than iron. Therefore, when the painted piping is measured using a UT, a coating thickness of about 2.5 times actual thickness is included in the pipe thickness. However, EMAR is unaffected by the presence of this coating.

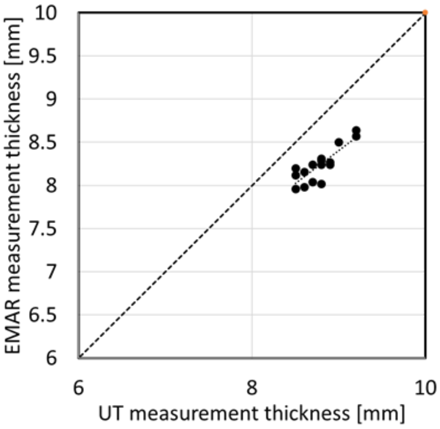

Fig. 19 Correlation between the measured EMAR and UT thicknesses.

5 Application of decommissioning plant to wall thickness monitoring

5.1 Outline of wall thickness monitoring system

The EMAR system is applied to evaluate its applicability for monitoring the pipe-wall thickness of the cooling system piping for the spent fuel pool circulation in the Fukushima Daiichi nuclear power plant (1F) Unit 4 [11-12]. The EMAR system consists of EMAT probes shielded by aluminum casing, a pulsar receiver (RPR-400, RITEC), a 10-CH probe switching device with a pre-amplifier, an A/D conversion unit for the FFT analysis (IDMS unit, Insight Co.), and a monitor PC. The pulsar receiver, A/D conversion unit, probe switching device, standard test pipe, and control PC are housed in a moisture-proof storage unit that is placed about 2 m away from the measurement-point locations.

The monitor PC remotely controls the system using the intra-company LAN from an administration building in a cold area. The probe switching device automatically switches the transmission/reception by the program. The burst wave is transmitted from the pulsar receiver, and the FFT spectrum intensity included in the reception signal is obtained by the A/D conversion unit.

The measurement positions are located on pipes downstream of an orifice where a reduction in thickness has been anticipated from the JSME S NH1-2006, a technical standard for pipe wall thinning of nuclear power plants [4]. Also, as a comparison, EMAT probes were set on pipes upstream of the orifice. Four EMAT probes were mounted circumferentially around the pipe wall at a 90° spacing. The EMAT probe is fixed with a resin band. Also, for standard test pieces, we measured the thickness of new pipes and detected an abnormality in the system.

The measurements of wall thickness were conducted once a day at a time specified automatically by the program. The wall thickness is obtained from measurement data using the SNC method. During measurement taking, the piping temperature is 5 to 30 °C., the space radiation dose is 0.2- 1.0mSv/h, and the piping surface radiation dose is 3.5 mSv/h.

5.2 Results and discussion

Figures 20 and 21 show the daily monitoring of pipe wall thickness downstream and upstream, respectively, of the orifice. Tables 2 and 3 list the certain results of these measurements. No significant change is noted in wall thickness due to thinning during the measurement period. However, the evaluation thickness downstream of the orifice has a variation of 0.3mm at maximum. Figures 22 and 23 show the results of the normalized SNC peak values downstream and upstream from the orifice. The normalized SNC peak value, an index reflecting the change in shape of the bottom surface, is stable at 0.2 or more upstream from the orifice. However, downstream from the orifice, its value is as low as 0.04.

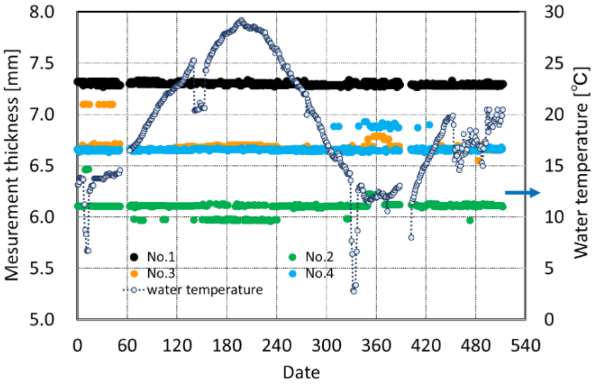

Fig. 20 Wall thickness monitoring results downstream of the orifice.

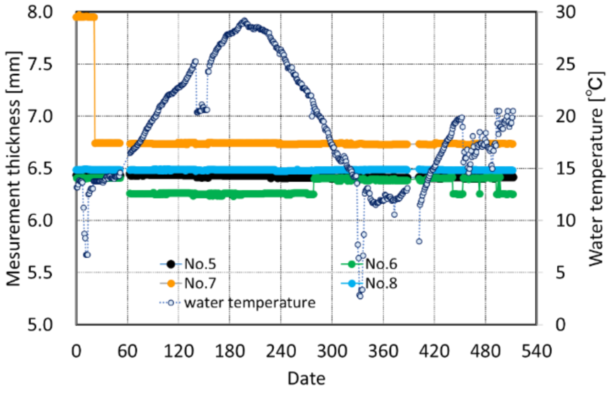

Fig. 21 Wall thickness monitoring process upstream of the orifice.

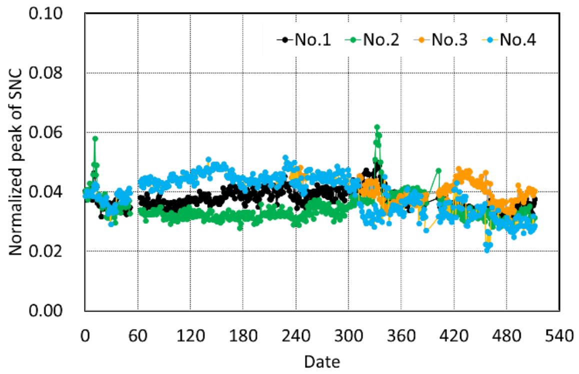

Fig. 22 Normalized SNC peak values downstream of the orifice.

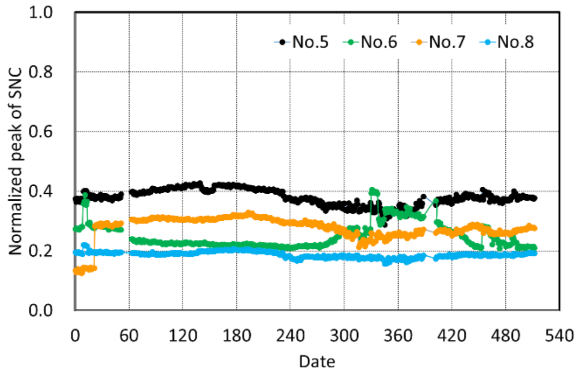

Fig. 23 Normalized SNC peak values upstream of the orifice.

Table 2 Downstream results of wall thickness measurements [mm].

	No. 1	No. 2	No. 3	No. 4
Initial thickness	7.30	6.10	6.66	6.67
512th day thickness	7.30	6.10	6.67	6.67
Minimum thickness	7.27	5.96	6.55	6.63
Maximum thickness	7.34	6.23	6.79	6.93

Table 3 Upstream results of wall thickness measurements [mm].

	No. 5	No. 6	No. 7	No. 8
Initial thickness	6.44	6.26	6.74	6.48
512th day thickness	6.42	6.25	6.74	6.48
Minimum thickness	6.40	6.24	6.72	6.47
Maximum thickness	6.44	6.42	6.75	6.49

In response to the accident, seawater and fresh water had been injected to cool the cooling system of Unit 4 [13]. Moreover, dust flew into the pool from the hydrogen explosion during the accident. In the breeding season, bacteria contained in the seawater secreted polysaccharide adhesive substances. Adhesive substances adhere to the inner wall of the pipe, fix suspended matter in the water to form slime and scale composed of microorganisms, organic matter, and inorganic matter.

Furthermore, together with dust, they form tuberculation on the inner surface of the pipe. Corrosion is accelerated by the potential difference between the tuberculation and its surroundings. In addition, bacteria enter the back of the tuberculation and become anaerobic promoting corrosion in the piping [14]. However, the measured thickness does not indicate occurrence of thinning. Therefore, the attenuation of the normalized SNC peak value of the orifice downstream is presumed to be caused by the attenuation of the ultrasonic wave due to the absorption and scattering at the interface between the inner surface of the pipe and also by these impurities adhering to the pipe.

Pipe wall thickness monitoring of the power plant unit in its decommissioning stage using the EMAR system has been continuous for over a year. Downstream from the orifice, the normalized SNC peak value is 1/5 or less compared with that upstream, the measured wall thickness being stable. However, a comparison of the variation in the measured wall thickness with previous measurement results has been possible as well as noise processing and smoothing. From the above, it is possible to apply the EMAT system to wall thickness measurements and provide monitoring of an actual plant.

6 Conclusion

The thickness of bent pipes of carbon steel that were actually used in a thermal power plant exhibiting FAC thinning from aged deterioration, was measured using EMAR and UT methods and a caliper gauge.

Moreover, the applicability of the EMAR method was evaluated through correlations between the measurement results of the three methods.

(1) At the initial stage of wall thinning, the inner surface was pitted by small indentation, but measuring the minimum wall thickness of these indentations using the EMAR and UT methods is difficult.
(2) Because the SNC peak value and FWHM depend on the shape of thinning, there is a possibility that thinning can be recognized at its initial stage.
(3) The FWHM on the periphery of maximum thinning is larger than that on the region of maximum thinning and the flat surface. If the FWHM obtained at a fixed point by EMAR monitoring is large, then there is a region where thickness reduction has progressed beyond the measurement point.

Second, the pipes of a thermal power plant during operation were measured using the EMAR method and its applicability evaluated. Sufficient measurements were possible. The difference with the UT method was 0.3–0.8mm but because the measurement was performed without removing the paint, this UT method included an additional thickness from the paint coating.

Finally, the EMAR monitoring system was applied in evaluating its applicability for monitoring pipe wall thickness pipes in the cooling system of the spent fuel pool circulation at the Fukushima Daiichi Nuclear Power Plant (1F) Unit 4. The monitoring of pipe wall thickness has been continuous for over 18 months. Downstream from the orifice, the normalized SNC peak value is 1/5 or less compared with that upstream, and the stability of the measured wall thickness was hindered. However, a comparison of the variation in measured wall thickness with previous measurements as well as noise processing and smoothing is possible. From the above, applying an EMAT system to wall thickness measurements and monitoring of an actual plant is viable.

Acknowledgement

We thank Mr. Kunihiro Kobayashi of Tohoku Electric Power Co., Ltd. for providing us with the FAC specimen and assistance in the EMAR measurement. We also thank Mr. Akinori Suzuki and Mr. Ryota Murayama of Tokyo Electric Power Holdings Inc. for their help in setting up the EMAR monitoring system at Fukushima Daiichi Nuclear Power Station.

References

[1] KOJIMA, F., KOSAKA, D., and UMETANI, K.: Continuous Surveillance Technique for Flow Accelerated Corrosion of Pipe Wall Using Electromagnetic Acoustic Transducer, AIP Conference Proceedings. AIP, Vol. 1335, No. 1, (2011), pp. 1341-1346.

[2] KOSAKA, D., KOJIMA, F., YAMAGUCHI, H., and UMETANI, K.: Monitoring system for pipe wall thinning management using electromagnetic acoustic transducer, E-Journal of Advanced Maintenance, Vol. 2, (2010), pp. 34-42.

[3] URAYAMA, R., UCHIMOTO, T., TAKAGI, T., and KANEMOTO, S.: Online Monitoring of Pipe Wall Thinning by Electromagnetic Acoustic Resonance Method, E-journal of Advanced Maintenance, Vol. 5, No. 5, (2013), pp. 155-164.

[4] TAKAGI, T., URAYAMA, R., ICHIHARA, T., UCHIMOTO, T., OHIRA, T., and KIKUCHI, T.: Field Application of Electromagnetic Acoustic Resonance to Inspection of Pipe Wall Thinning in a Nuclear Power Plant, Studies in Applied Electromagnetics and Mechanics, Vol. 38, (2014), pp. 312.

[5] URAYAMA, R., TAKAGI, T., UCHIMOTO, T., KANEMOTO, S., OHIRA, T., and KIKUCHI, T.: Implementation of electromagnetic acoustic resonance in pipe inspection, E-journal of Advanced Maintenance, Vol. 5, No. 1, (2013), pp. 25-33.

[6] SEHER, M., and NAGY, P.B.: On the separation of Lorentz and magnetization forces in the transduction mechanism of Electromagnetic Acoustic Transducers (EMATs), NDT & E International, Vol. 84, (2016), pp. 1-10.

[7] HIRAO, M. and OGI, H.: EMATs for science and industry: noncontacting ultrasonic measurements, Springer Science & Business Media, 2013.

[8] URAYAMA, R., UCHIMOTO, T., TAKAGI, T., and KNEMOTO, S.: Quantitative evaluation of pipe wall thinning by electromagnetic acoustic resonance, E-Journal of Advanced Maintenance, Vol. 2, (2010), pp. 25-33.

[9] ABE, H., WATANABE, Y., NAKASHIMA, M., and TATSUKI, Y.: Characterization of the corroded surface

morphology of a carbon steel piping elbow affected by flow-accelerated corrosion, E-Journal of Advanced Maintenance, Vol.9, No. 1, (2017), pp. 26-32.

[10] SUN, H., URAYAMA, R., UCHIMOTO, T., KOJIMA, F., TAKAGI, T., ABE, H., KOBAYASI, K.: "Effect of Scaly Structure on the Measurement of Pipe Wall Thickness using EMAT", E-Journal of Advanced Maintenance, Vol.9 No.1 (2017) pp. 15-25.

[11] TAKAGI, T., UCHIMOTO, T., URAYAMA, R., and SUZUKI, A.: Application of monitoring system using electromagnetic acoustic transducers for wall thickness measurement to Fukushima Daiichi nuclear power plant unit 4 spent fuel pool cooling piping, Japan Society of Maintenology, Proceedings of the 14th Annual Conference, (2017), pp. 489-490. (Japanese)

[12] TAKAGI, T., UCHIMOTO, T., URAYAMA, R., and SUN, H.: Wall thickness measurement of piping using electromagnetic acoustic resonance method and its application to nuclear reactor cooling system, Japan Society of Maintenology, Proceedings of the 15th Annual conference, (2018), pp. 149-150. (Japanese)

[13] INOUE, M., and ASAKA, T.: Temperature and Chemical History of Spent Fuel Pools in Fukushima Daiichi Nuclear Power Station: Units 1 through 4, JAEA-Review 2014-020. (Japanese)

[14] KIKUCHI, Y., and SREEKUMARI, K.R.: Microbially Influenced Corrosion and Biodeterioration of Structural Metals, Tetsu-to-Hagane, Vol. 88, No. 10, (2002), pp.34-42 (Japanese)